JOURNAL OF AIRCRAFT
Vol. 47, No. 4, July–August 2010

Airspace Constraints in Aircraft Emission Trajectory Optimization

Marianne Jacobsen* and Ulf T. Ringertz*
Royal Institute of Technology, 100 44 Stockholm, Sweden

DOI: 10.2514/1.47109

This paper describes a method for handling restricted airspace in trajectory optimization problems while maintaining the full dynamics of the aircraft model. The discussion is limited to the local solution of the optimization problem. The topological problem of determining which side of the restricted regions the aircraft trajectory should take can be seen as more of a preprocessing stage that determines, for example, the shortest path. The trajectory optimization is performed with environmental objective functions describing the emissions from the aircraft engine. Results from two cases are presented. The first case is flying in the vicinity of an airport during the approach and avoiding flying directly above urban areas. The second case involves a long-distance flight with a large region of restricted airspace in the way. Both cases are performed with a model of the Swedish Air Force trainer SK60. The results show that the solution and the solution time significantly depend on the initial starting guess. With a feasible starting guess, the efficiency of the optimization algorithm is not too degraded by the nonconvex airspace constraints.

I. Introduction

AIRCRAFT trajectory optimization has been studied for several decades, and many important and interesting problems have been considered, such as finding the trajectory that minimizes the time to climb [1] or maximizes the final fuel mass [2]. For military purposes, Norsell [3] showed the possibility of including radar-range constraints and also minimizing the detection time during a mission. Trajectory optimization is not only used for aircraft, but several space applications have also been reported. Betts [4], for example, discussed the challenging problem of controlling the low-thrust trajectory of a spacecraft. Noise is also being considered as an objective function and has recently been studied for a helicopter by Tsuchiya et al. [5].

Computing the aircraft trajectory can be formulated as an optimal control problem, and several solution methods for this type of problem exist and are discussed by Betts [6], among others. In the work presented here, the problem is discretized and formulated as a nonlinear programming problem. In many applications, the full six-degree-of-freedom model can be reduced to only consider longitudinal degrees of freedom. In some situations, however, this reduces the accuracy too much and a three-dimensional model is required. Examples may be found in military applications when flying through specified waypoints and not violating restricted airspace or so-called no-fly zones [7]. Civil applications may include the three-dimensional trajectory of an aircraft on approach for landing.

In the above applications, airspace constraints need to be treated. Adding a geometrical constraint on the trajectory can be a nonconvex constraint if it removes parts of the interior of the feasible region. This may make the problem much more difficult to solve, and only a local solution to the problem is generally found. Also, if a nonlinear programming approach is used, all derivatives should at least be continuous. This study focuses on the treatment of restricted regions in the trajectory optimization problem. A circular restricted airspace simplifies the formulation of the constraints, since it can be written in closed form with continuous derivatives, which has been treated by Jorris and Cobb [7] and Eele and Richards [8].

Restricted airspaces are generally of two kinds: either a circular region or a polygon. The polygons can, in turn, be either convex or nonconvex. Staying inside a circle or a convex polygon is straightforward and a convex problem. This problem is also of importance, for example, during a climb in which the aircraft has a limited space in which to perform the maneuver, as discussed by Dai and Cochran [9].

II. Aircraft Performance and Trajectory Optimization

The equations governing the motion of an aircraft can be reduced from the full six-degree-of-freedom model [10] using a point-mass model of the aircraft and assuming a flat-Earth frame of reference. The resulting equations that have been used in this study are of the form

$$m\dot{V} = T\cos(\alpha + \epsilon) - D - mg\sin\gamma \tag{1}$$

$$mV\dot{\gamma} = T\sin(\alpha + \epsilon)\cos\phi + L\cos\phi - mg\cos\gamma \tag{2}$$

$$mV\dot{\psi}\cos\gamma = T\sin(\alpha + \epsilon)\sin\phi + L\sin\phi \tag{3}$$

$$\dot{h} = V\sin\gamma \tag{4}$$

$$\dot{m}_f = -b \tag{5}$$

$$\dot{x}_E = V\cos\gamma\cos\psi \tag{6}$$

$$\dot{y}_E = V\cos\gamma\sin\psi \tag{7}$$

and have been derived by Ringertz [2] and also used with satisfying results by Norsell [3]. Here, m is the total mass of the aircraft, m_f is the fuel mass, b is the fuel burn, V is the speed of the aircraft, T is the engine thrust, L is the lift, and D is the drag. The gravity acceleration is denoted as g. The angles of importance in the model are the angle of attack α; the thrust angle with respect to the body axis, ϵ; and the flight-path angle γ. The bank angle is ϕ and the heading is ψ. The heading is measured clockwise from the north direction. The position of the aircraft is given by the altitude h as well as the coordinates x_E and y_E, where the subscript E denotes Earth coordinates. For the atmospheric data, the standard atmosphere is assumed. This model is referred to as a 3-D model of the aircraft.

Received 9 September 2009; revision received 5 November 2009; accepted for publication 5 November 2009.

*Department of Aeronautical and Vehicle Engineering, Division of Flight Dynamics.

Commonly, these equations are reduced to a 2-D longitudinal model when trajectory optimization is performed. When long distances are considered, the bank-angle dynamics are usually negligible. However, in the case of an aircraft on approach for landing or when an obstacle or no-fly zone needs to be avoided, the 3-D dynamics may be of importance.

A. Aircraft Model

The aircraft in this study is the Swedish Air Force trainer Saab 105, or SK60 (see Fig. 1). The aircraft is modeled with great detail, such as Mach number dependencies of all aerodynamic coefficients. The aerodynamic coefficients, as well as the engine, are modeled using least-squares fits of *B*-spline basis functions [11] to tabular data, making the evaluations efficient and smooth. The aircraft model is described in more detail in Appendix A and in Ringertz [12]. In this study, the clean-aircraft configuration is modeled, making it difficult to simulate the entire approach in the optimization problem, since that would require airbrakes, flaps, and landing gear. These are not easily modeled as continuous variables, however, and are not used in this study. Instead, the aircraft trajectory is only computed to a final approach point located approximately 1 km from the runway.

The engine on the SK60 is an FJ44 from Williams International. Using the International Civil Aviation Organization certification data [13], the emissions can be modeled with smooth *B*-splines (see Fig. 2). The emission indices used here are those from the certification data, i.e., carbon monoxide (EICO), hydrocarbons (EIHC), and nitrogen oxides ($\mathrm{EINO_x}$). The emissions as a function of altitude and Mach number are modeled using the Boeing fuel flow method 2 [14]. These emissions may be used as objective functions in the optimization problem or as weighted sums to form different environmental indices as used in life-cycle impact assessment (described by Baumann and Tillman [15]). The environmental indices can be acidification or human toxicity potential or more general indices such as the Eco-indicator'99 [16].

Fig. 1 SK60 aircraft (copyright Saab AB, photographer Peter Liander).

B. Discretization and Nonlinear Programming

The equations of motion (1–7) of the aircraft can be written in compact form as a system of first-order differential equations:

$$\dot{x} = f(x, u) \tag{8}$$

where $x = (V \quad \gamma \quad \psi \quad h \quad m_f \quad x_E \quad y_E)^T$ is the vector of state variables, and $u = (\alpha \quad \phi \quad \delta_p)^T$ is the vector of controls, with δ_p denoting the throttle setting. To this set of equations, algebraic constraints such as limiting load factor are added. The load factor in this study is limited to vary between -3 and 6. The equations are discretized in time using Hermite–Simpson collocation [17], and the discretized states at all time steps are gathered in the variable vector y. Choosing a proper objective function $f(y)$, such as the final time or final fuel mass, a nonlinear programming problem may be posed as

$$\min_y f(y) \tag{9}$$

$$\text{subject to } \underline{l} \le \begin{pmatrix} c(y) \\ Cy \\ y \end{pmatrix} \le \bar{u} \tag{10}$$

where the discretized equations of motion and the algebraic limitations are used as constraints $c(y)$. Here, f denotes the scalar-valued objective function and y are the discretized state and control variables. The matrix C may define linear continuity constraints if the problem is defined using a multistage formulation (see Ringertz [18]). The vectors containing the lower and upper bounds of the constraints are denoted as $\underline{l}$ and $\bar{u}$, respectively.

To solve this nonlinear programming problem, the solver SNOPT [19] is used. It is an efficient sequential quadratic programming algorithm that solves a quadratic subproblem in each iteration. The algorithm uses quasi-Newton approximations to the required second-derivative information, and it efficiently exploits sparsity in the constraint Jacobian when solving the quadratic subproblem. Exploiting sparsity is important, since the discretized problem may become quite large, especially if range problems are considered.

III. Airspace Constraints

Restricted airspace can be of different types: for example, military practice regions, bird protection areas, or nuclear power plant surroundings. Generally, these areas are either described by circular regions or by polygons on the map. Adding these constraints to the nonlinear optimization problem will be in the form of constraints on the state variables x_E and y_E. Removing parts of the feasible region with restricted airspace may make the problem more difficult, due to nonconvexity. It is also desired to have continuous first derivatives of all constraints in the optimization problem.

When restricted airspace is added to the problem, finding the solution can be divided into two main parts. In this study, the topological route is first decided, since there will be local solutions on each side of the airspace. Hence, the solution will depend quite heavily on the initial starting guess using the proposed method in this

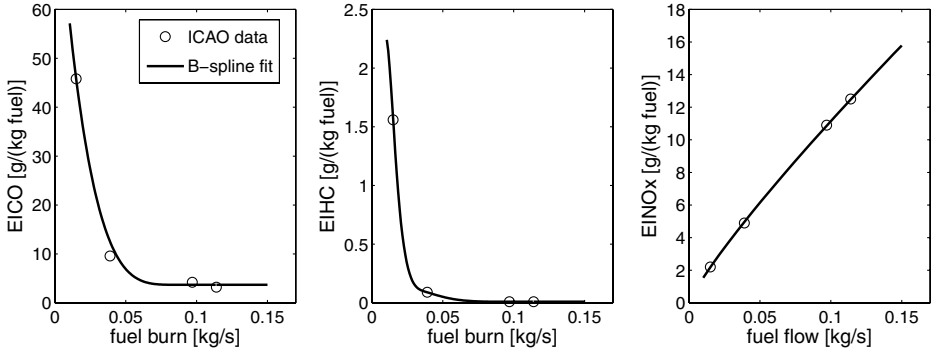

Fig. 2 Emissions from the FJ44.

study. The topological problem could be solved using, for example, a branch-and-bound technique, as described by Eele and Richards [8], or the Voronoi diagram technique described by Judd and McLain [20]. When the topological route has been determined, the nonlinear programming problem is solved with the geometrical constraints to find the locally optimal solution.

A. Circular Airspace

Adding circular regions as constraints is rather straightforward, even though the resulting problem may become difficult to solve. A circular constraint can be added as one constraint in each time step at which the geographical variables at that time step, x_E and y_E, must lie at least a distance R from the center of the circle. Using circular constraints in trajectory optimization has been described and tested previously: for example, by Eele and Richards [8] and Jorris and Cobb [7]. The problem is also closely related to the radar-range constraints discussed by Norsell [21].

A more adaptable shape is the ellipse. The constraint for each time step become similar to staying outside the circle if the ellipse is written in general (center) form as $(x-c)^T E(x-c) = 1$. Here, $x \in \mathbb{R}^2$, and $c \in \mathbb{R}^2$ denotes the center of the ellipse. The matrix E should be symmetric positive definite, i.e., $E = E^T \succ 0$. Ellipses are used as constraints in Jorris et al. [22].

B. Polygon-Shaped Airspace

Staying inside a convex polygon can be formulated as linear constraints in the form of $Ax \leq b$, but in the case of staying outside the polygon, the formulation is not given by $Ax \geq b$. Since the description of the region is to be used in optimization, a smooth curve with continuous first derivatives is desirable. The problem studied here is, therefore, how the polygon can be approximated with a smooth curve that may be used as a constraint in the optimization problem, as done with the circular region above.

A polygon airspace constraint can be both convex and nonconvex. Here, only the convex case is considered, since the nonconvex polygon can be divided into two or more convex polygons (see Fig. 3, in which the interior of the polygon represents the restricted airspace or no-fly zone). A general convex polygon consists of a set of points constituting the corners of the polygon. For the application with airspace constraints, the number of corners is not assumed to be very large: rather, in the vicinity of 5–10. The problem is now to approximate the polygon with a smooth curve. The approximation should, of course, be as similar as possible to the original shape, but a requirement on the approximation is that it should always be outside the original polygon, making sure that the optimal trajectory will not pass through the restricted airspace. There are several different alternatives for the approximation. Here, a few are discussed and methods for finding the approximations are described.

The simplest case would be to enclose the polygon within a circle. The circle can then be used as described previously. Finding the smallest circle can be done in several ways, and different solutions to the problem are discussed by Xu et al. [23]. If the polygon is rather rectangular in its shape, the smallest enclosing circle may be quite large; in this case, an ellipse may be more suitable. If the ellipse is given in the general form of $(x-c)^T E(x-c) = 1$, the problem of finding the minimum ellipse enclosing the points p_i can be formulated as

$$\min_{E,c} \det(E^{-1}) \tag{11}$$

$$\text{subject to } (p_i - c)^T E(p_i - c) \leq 1, \quad \forall\ i \tag{12}$$

$$E \succ 0 \tag{13}$$

where $\det(E^{-1})$ denotes the determinant of the inverse of the matrix E. This property is proportional to the volume, or area in 2-D, of the ellipse. This problem is nonconvex, but following the method described by Kumar and Yildirim [24], the problem can be solved using the Khachiyan first-order algorithm [25].

Yet another approach would be to discretize the polygon into smaller regions and cover each region with a circle (or ellipse). This strategy is proposed by Eele and Richards [8]. The most apparent drawback is that a single polygon constraint will result in several circular constraints, making the number of constraints in the optimization problem increase dramatically if the original shape of the polygon should be somewhat preserved.

In the application with restricted airspace, it may not be important to fly as close to the airspace as possible, but rather to guarantee that the trajectory is outside the region (see Raghunathan et al. [26]). The proposed method for handling polygon-shaped constraints in this study is to keep the shape of the polygon and remove the sharp corners by adding small circles of constant radius around the corners. The circles are connected with lines that are parallel to the polygon sides; this will give regions, as shown in Fig. 4.

To use the above shape as a constraint, a distance function $f_d(x_E, y_E)$ needs to be defined. It should be chosen, for example, to be positive for points outside the polygon and negative for points inside the polygon. The computation of this distance should also be as simple as possible and preferably without any iterations, since this will be computed during the optimization. Also, the derivatives of the distance function should be easily determined. This problem is solved by regarding the flat polygon shape as a contour line of a three-dimensional function. This 3-D function can be constructed by computing the coordinates of the center point of the polygon as the mean of all corner x and y coordinates and assuming that this center point has a z coordinate of $z = 0$. This center point can then be moved in the negative z direction to a point V_c. This new point is used to construct the 3-D function as follows. The circles around the corners in the 2-D plane are extracted to form tilted cones with vertices in V_c. Then the lines connecting the circles in Fig. 4 are made into planes passing through V_c; this is illustrated in Fig. 5.

The distance function $f_d(x_E, y_E)$ to the smooth polygon is now defined as the z coordinate of the surface in Fig. 5 at a point p given by $p = (x_E, y_E, 0)^T$. This z coordinate should not be confused with the altitude of the aircraft, which is not part of this discussion. If p is inside the polygon, the z coordinate of the surface will be negative (hence, a negative distance is obtained), and a positive distance will refer to a point outside the polygon. This gives a simple constraint to

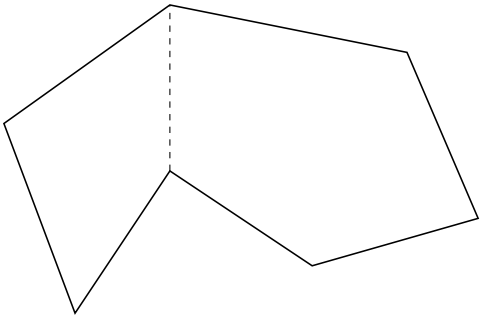

Fig. 3 Nonconvex polygon split into two convex polygons.

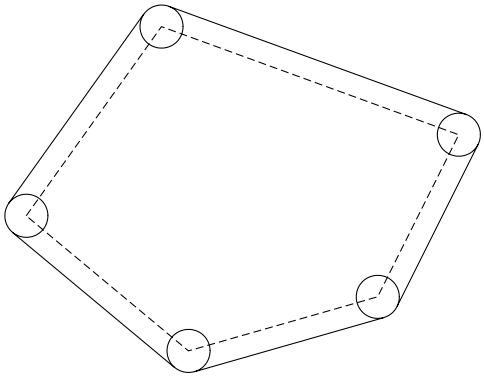

Fig. 4 Making a smooth curve out of a polygon.

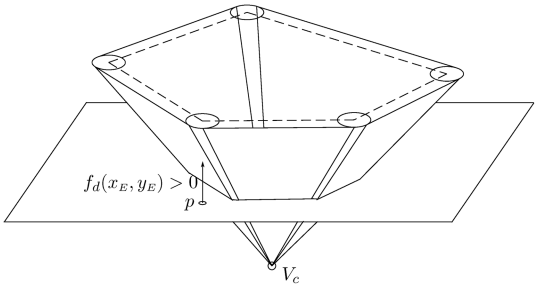

Fig. 5 Three-dimensional surface with contour lines of the smooth polygon.

the optimization problem that states that this distance should be positive at all time steps, i.e., $f_d(x_E, y_E) \geq 0$.

The evaluation of the distance function involves different steps. First, it must be decided if the desired distance should be computed as the z coordinate of a plane or of a cone and also which plane or cone should be used, which means determining in what region the point p is located. The different regions are illustrated with dashed–dotted lines in Fig. 6. As seen here, the regions can be described by linear inequalities, meaning that it is rather efficient to determine where the point is located. There are two general cases: either the distance should be computed to a plane or to a cone. If the surface in the current region is a plane, it is straightforward to find the desired z coordinate. Assume that the chosen plane is described by

$$ax + by + cz + d = 0 \tag{14}$$

At $p = (x_E, y_E, 0)$, the distance function, i.e., the z coordinate of the plane 14, can be evaluated as

$$f_d = \frac{-(ax_E + by_E + d)}{c} \tag{15}$$

This will be positive when p is outside the polygon and negative when inside. The derivatives with respect to the state variables x_E and y_E of the distance are simply

$$\frac{\partial f_d(x_E, y_E)}{\partial x_E} = -\frac{a}{c} \tag{16}$$

$$\frac{\partial f_d(x_E, y_E)}{\partial y_E} = -\frac{b}{c} \tag{17}$$

The regions in which the distance should be computed to a cone instead are evaluated similarly, but in this case the distance will be given by a second-degree equation. The desired distance is always the minimum of the two solutions, which works for points both interior of the polygon and outside. The problem can be formulated as finding the intersection of the cone given by

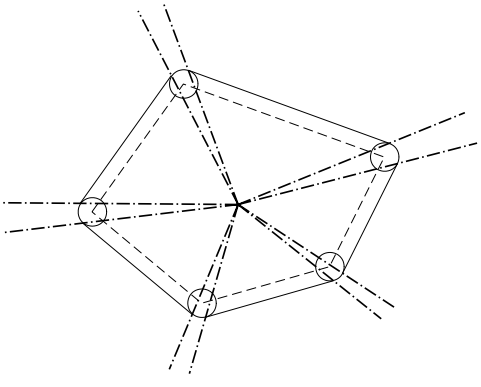

Fig. 6 Regions that determine which distance should be computed.

$$\left(x - x_c - \frac{z}{z_{\text{vc}}}(x_{\text{vc}} - x_c)\right)^2 + \left(y - y_c - \frac{z}{z_{\text{vc}}}(y_{\text{vc}} - y_c)\right)^2 = \left(\frac{r}{z_{\text{vc}}}(z - z_{\text{vc}})\right)^2 \tag{18}$$

and the line given by

$$x = x_E, \qquad y = y_E \tag{19}$$

where (x_c, y_c) is the center point of the circle with radius r around the polygon corner, and $V_c = (x_{\text{vc}}, y_{\text{vc}}, z_{\text{vc}})$ is the vertex of the cone. The derivatives also become closed form expressions.

A parameter that can be chosen somewhat arbitrarily is the z coordinate of the vertex V_c, as defined previously. If it is chosen far from $z = 0$, the 3-D surface (planes and cones) will be very steep resulting in rather large distances for points far outside the restricted region. Depending on how the constraints are defined in the optimization software, this may be a problem. In SNOPT, the constraints are defined with both upper and lower bounds, meaning that the upper bound needs to be chosen sufficiently large in order for the points not to be restricted to be close to the airspace constraint. The distance to the airspace constraint will be smaller if the z coordinate of V_c is chosen closer to zero since the cone will be less steep in this case.

The altitude in the trajectory optimization problem has not been included in the definition of these restricted areas but only the geographical coordinates x_E and y_E. Typically, these no-fly zones also have an altitude interval in which they are active, but for the case of coming in for landing and not flying directly over cities, this should hold for all altitudes of interest in the problem. Many of the military practice regions also have very high altitude limits, making it nonrealistic to fly above the regions instead of flying around them.

IV. Results

The restricted airspace constraints are implemented as algebraic constraints in the FORTRAN code for the trajectory optimization using SNOPT as the optimization solver. Each region results in one nonlinear constraint for each time step; this does not affect the efficiency of the optimization solver too much, even though the problem may be more difficult to solve. The importance of the initial starting point for the solver is also increased, due to the nonconvexity of the airspace constraints.

The first case studied here is the approach of an SK60 to Malmen outside Linköping in Sweden. The airport is located close to several smaller cities, giving constraints on the approach. The trajectory should not pass through urban airspace to reduce noise and emissions. The first case is a short flight, but with several constraints. The second case is more of a long-distance flight. Here, the starting point is chosen outside Stockholm and the finish is at Visby on the island of Gotland. Between these two cities, there is a large region of restricted airspace where air traffic is prohibited with an altitude limit of approximately 12 km.

A. Approach to Malmen

The region around Malmen is studied and polygon-shaped regions are fitted to the urban areas in the neighborhood. These can easily be constructed from Global Positioning System (GPS) coordinates on a map. To translate the GPS coordinates to a flat Earth coordinate system, the MATLAB package M_Map [27] is used with a Mercator projection. These coordinates are used to build restricted airspace regions used as constraints in the optimization.

Since the final part of the approach is preparations for touchdown, this part of the flight is left out of the optimization. Here, the pilot would need to use the flaps and also extend the landing gear to prepare for landing. Therefore, the final conditions for the optimization is set at a point approximately 1 km from the runway at an altitude of 180 m. This point is chosen by studying GPS data from the approach performed by several military pilots in the SK60. At this point, all

Table 1 Initial and final conditions for the approach to Malmen

Variable	Initial	Final
V, m/s	150	80
h, m	900	180
m_f, kg	670	Maximum
ψ, deg	free	198

flights available show the aircraft lined up with the runway at 180 m with decreasing speed.

One of the flights performed with the SK60 is chosen to obtain realistic altitude and speed data for a starting point approximately 40 km east of Malmen. The initial and final conditions of the trajectory are given in Table 1. The objective function is chosen to maximize the remaining fuel mass from a fixed initial fuel mass, resulting in a minimum-fuel-burn trajectory. The fuel-optimal trajectory is shown in Fig. 7 together with the path of the real SK60 flight.

Some of the state and control variables of the trajectory are shown in Fig. 8. The throttle setting δ_p is defined to vary between 0.31 (flight idle) and 0.87 (full thrust). The altitude first increases up to approximately 2 km with full throttle and after about 35 s flight idle is chosen. The speed is slowly reduced throughout the flight, but almost constant during the slow dive with the throttle in idle. The bank angle

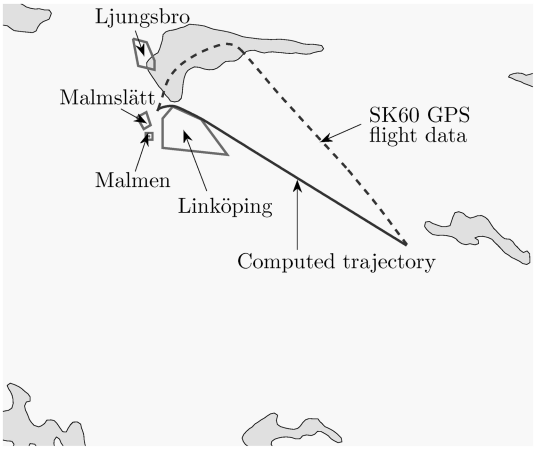

Fig. 7 Fuel-optimal trajectory on approach for landing (solid) and SK60 GPS flight path (dashed).

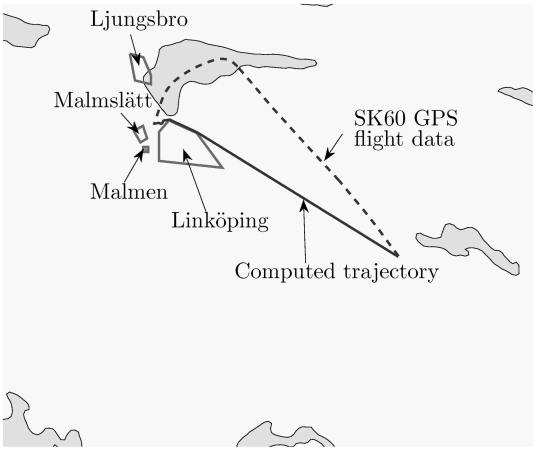

Fig. 9 HTP optimal trajectory on approach for landing (solid), SK60 GPS flight path (dashed).

is a control variable and is chosen almost zero for the most part of the flight. When the restricted airspace over Linköping is encountered, the bank angle is increased to stay outside the region. The bounds on the bank angle are set to $-80^\circ \leq \phi \leq 80^\circ$. The bank angle is rather large in the final turn when the aircraft is lining up with the runway; this is due to the objective function. Minimizing the fuel burn will give as short of a distance as possible, making it optimal to make a very steep turn at the end instead of taking a longer path with a smaller bank angle. The steep turns can be controlled by reducing the bounds on the bank angle if a trajectory with a smaller load factor is desired.

The minimum-fuel-burn trajectory results in the same trajectory as if carbon dioxide is minimized. Carbon dioxide adds to global warming and it is an important emission to reduce. However, in the vicinity of airports, people are living close to where aircraft fly and also close to the emissions. Aircraft on approach for landing, or taking off, are flying close to the ground and emissions from the engines are likely to affect people and nature more than when flying high in the atmosphere. Therefore, it may be interesting to minimize the toxic emissions that are affecting humans considerably. An index known as *human toxicity potential* (HTP) can be defined by putting weights on the different emissions in the engine exhaust [15,28]. The index is linear in the emissions, but the actual emissions are nonlinear due to the Boeing fuel flow method as used in this study. This index can be used as the objective function, instead of the fuel burn, in the

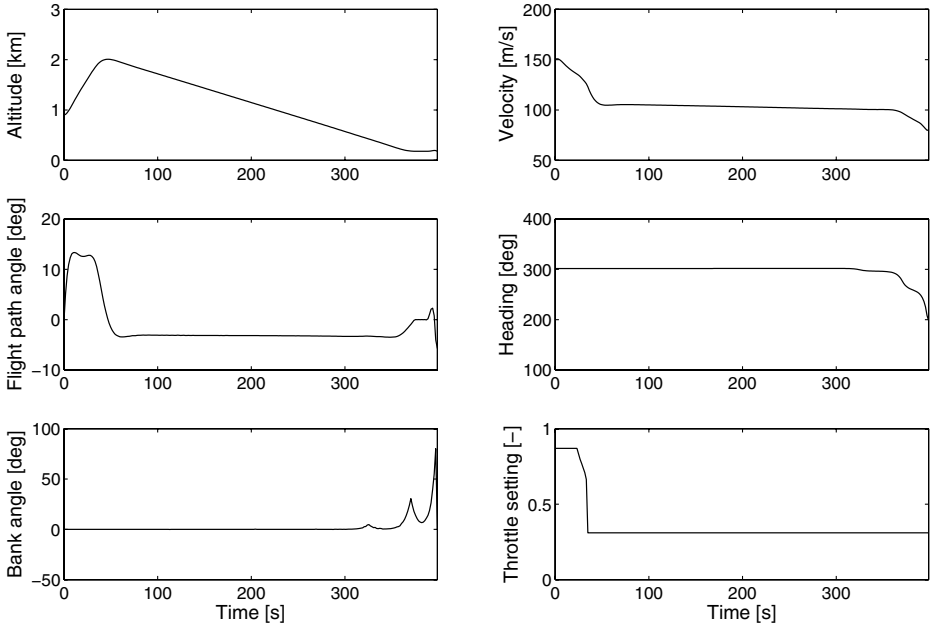

Fig. 8 Control and state variables for the fuel-optimal flight path.

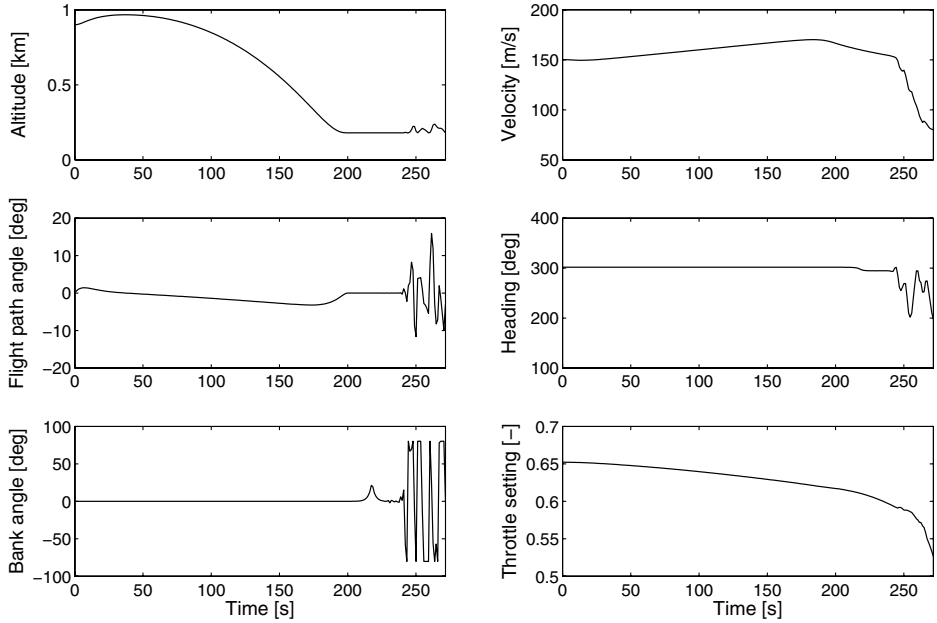

Fig. 10 Control and state variables for the HTP optimal flight path.

trajectory optimization problem. The same constraints, initial and final conditions are used, and the HTP optimal flight path is shown on the map in Fig. 9. The state and control variables are shown in Fig. 10.

The geographical trajectory in Fig. 9 looks rather similar to the fuel-optimal trajectory, but looking at the state and control variables, some significant differences can be seen. The HTP optimal trajectory is a lot shorter in time. It takes approximately 275 s instead of 400 s to complete the task. The throttle is now kept significantly higher to avoid flight idle where the combustion is inefficient emitting high quantities of mainly hydrocarbons (HC) and carbon monoxide (CO) (see Fig. 2). These emissions are toxic and are thus weighted heavily in the HTP index. The HTP value for this trajectory is 0.59, which should be compared to the HTP value for the fuel-optimal flight path, which is 2.22. Hence, minimizing HTP instead of fuel burn results in a 73% decrease in the HTP value. However, the fuel used during the approach is increased significantly, from 24.5 kg for the fuel-optimal trajectory to 36.9 kg, corresponding to an increase of 51%.

Another environmental index is the Eco-indicator'99 [16]. Here, different weights are put on all emissions and the weighted sum is computed to form an environmental index designed to describe the total environmental impact of a process. The Eco-indicator'99 is also used as the objective function in the approach problem to Malmen using the same constraints and initial and final conditions as for the previous cases. A comparison of the state and control variables is shown in Fig. 11 for the different objective functions. The Eco-indicator'99 solution is similar to the fuel-optimal trajectory, but the speed is lower, making the time to complete the approach longer. The throttle setting is also quite different from the fuel-optimal trajectory, which is most likely an effect of the other emissions that are increased significantly for low throttle settings. The amount of fuel used is only slightly increased from the 24.5 kg used in the fuel-optimal trajectory to 25.6 kg for the Eco-indicator trajectory. The Eco-indicator index is reduced from 0.84 to 0.77 when comparing the fuel-optimal trajectory and the Eco-indicator trajectory.

The HTP optimal solution in Fig. 10 may look strange with very large variations in mainly the flight-path angle γ and the bank angle ϕ. The optimality of this solution can be questioned, but optimality can be checked by studying the projected Hessian of the Lagrangian:

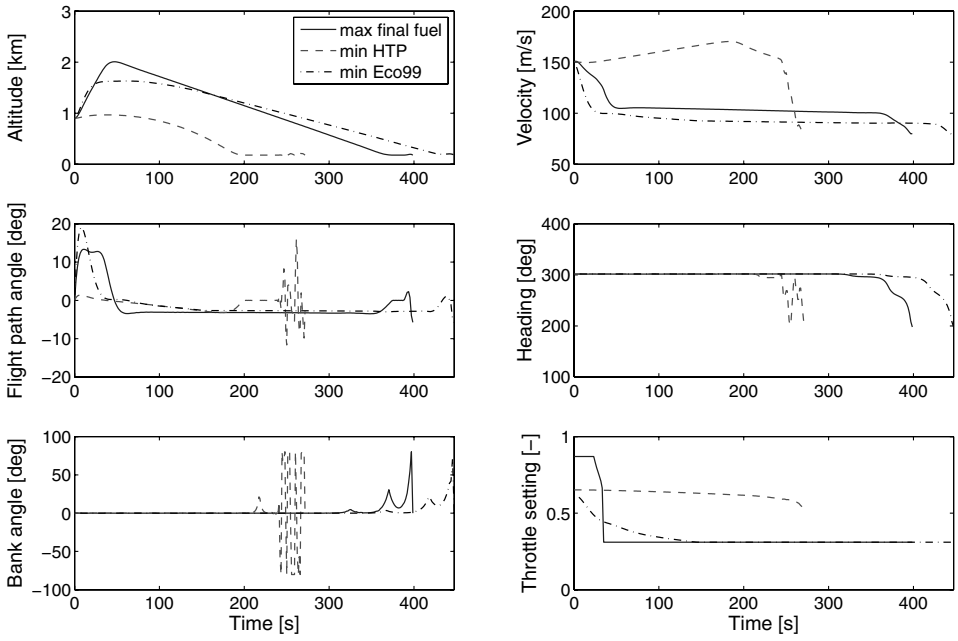

Fig. 11 Control and state variables for the different objective functions.

Table 2 Initial and final conditions for the Visby trajectory

Variable	Initial	Final
V, m/s	150	90
h, m	500	180
ψ, deg	free	20

$$Z^T L Z \succ 0 \tag{20}$$

where Z is a basis for the null space of the active constraints at the solution, $L = \nabla^2 l(x, \lambda)$ is the Hessian of the Lagrangian $l(x, \lambda)$, and $\succ$ denotes positive definite. The Lagrangian is defined here as

$$l(x, \lambda) = f(x) - \lambda^T c^*(x) \tag{21}$$

with $f(x)$ as the objective function, $c^*(x)$ as the active constraints, and λ as the vector of Lagrange multipliers. The Hessian of the Lagrangian can be computed from the output of SNOPT using finite differences on the first derivatives of the objective function and the active constraints. The projected Hessian of the Lagrangian should be positive definite if the solution is an optimum. This was found to hold for the oscillating solution in Fig. 10, and considering the objective function it may very well be optimal to keep the throttle high for as long as possible. However, this results in a lot of extra kinetic energy of the aircraft, which somehow needs to dissipate when the speed should be reduced at the end of the flight. Therefore, the aircraft starts to oscillate to reduce the energy and also the speed. This is not a desirable solution from a pilot perspective, but rather an artifact from the mathematical model of the aircraft and the solution method that solves the mathematical optimization problem as posed. There are several simplifications in the modeling adding to this behavior. For example, the roll rate in the model is assumed infinite, making large variations in the bank angle in zero time possible. Also, no time delay between throttle setting and thrust is modeled. The same oscillating behavior is seen when the final time is used as objective function. This problem can be resolved, for example, using the method described in Jorris et al. [22], where control rates are used rather than control angles to avoid the infinite roll rates.

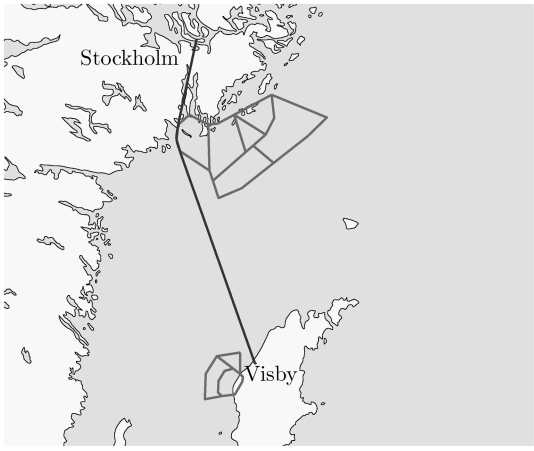

Fig. 12 Fuel-optimal long-range trajectory with airspace constraints.

B. Stockholm to Visby

The previous case was a short flight, but here, a more long-distance case is studied. To capture the dynamics of the aircraft, the discretization should not be too coarse, making the problem rather large when a long-distance flight is studied. The chosen case is a flight from Stockholm to Visby, a distance of about 200 km. In between Stockholm and Visby, there is a large area of restricted airspace up to an altitude of 12 km. Outside Visby there is another large region of restricted airspace also added to the trajectory optimization problem. The aircraft is assumed to land on a runway at a 20° heading. The initial and final conditions for the flight are given in Table 2.

Since this is a long-distance flight and the final conditions are again given by a low speed, an appropriate objective function is maximizing the final fuel, i.e., using as little fuel as possible. The restricted airspace is in this case given by some nonconvex regions, and these are first divided into convex polygons to make sure the method described here will work. The optimal trajectory is shown on the map in Fig. 12. The state and control variables are shown as the solid lines in Fig. 13.

The problem is difficult to solve with the large restricted area, but using a feasible starting guess makes it possible to find a solution rather efficiently. The altitude increases to 7.8 km and the throttle is kept at its maximum before reducing it all the way to flight idle after about 500 s. Again, the distance of the trajectory largely affect the fuel burn, making the final turn very steep.

The same problem is solved again using the Eco-indicator'99 as the objective function, and a comparison between the state and

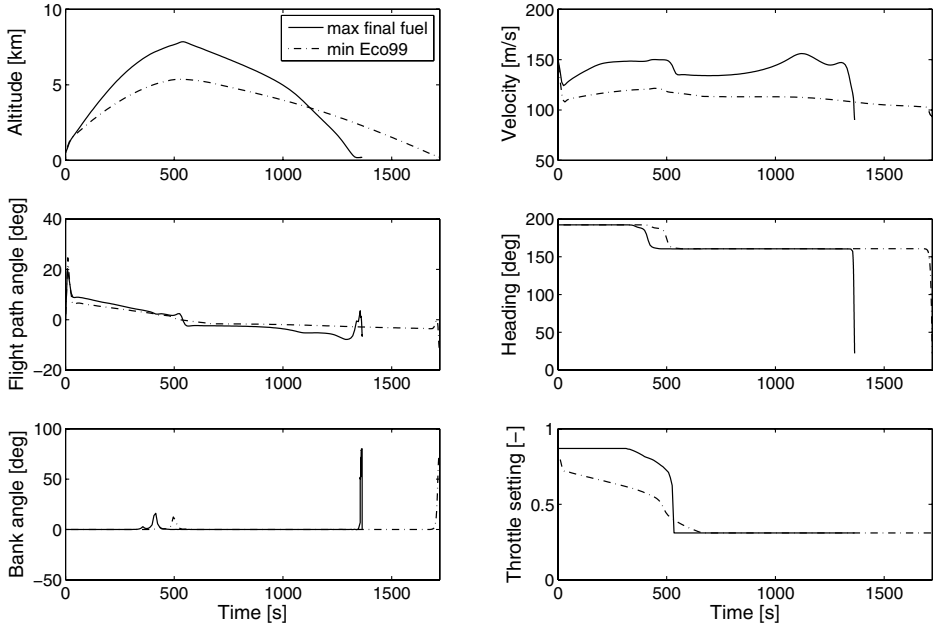

Fig. 13 State and control variables for the Stockholm to Visby case.

control variables for the different objective functions are shown in Fig. 13. There is a significant difference between the two solutions. The speed is lower and the altitude is not increased as much in the beginning of the flight. On a long flight like this, the use of the HTP index is questionable since it only takes into account the emissions that are related to human health and not the environment as a whole. It is, therefore, not shown here. The Eco-indicator index is reduced from 4.72 in the fuel-optimal trajectory to 4.38 when used as the objective function, a decrease of approximately 7%. On the other hand, the amount of fuel used during the flight is increased from 117 kg for the fuel-optimal flight to 124 kg for the Eco-indicator optimal flight, which corresponds to approximately 6.5%.

V. Conclusions

The solution of a three-dimensional trajectory optimization problem has been studied. The method discussed makes it possible to formulate the trajectory optimization problem with restricted airspace. When the airspace is described by circular regions the formulation is straightforward even though the resulting problem may be difficult to solve even with high performance optimization techniques. However, a polygon is a common shape of restricted airspace. In this case, no simple formulation exists. The solution to this problem, as presented here, is to round the corners of the polygon and extract the 2-D region to a 3-D surface with contour lines as the shape of the restricted area. The main advantage of this approach is that only one constraint will be added for each time step instead of covering the region with circles resulting in several nonlinear inequality constraints.

The constraints are added to make each point in the discretized path lie outside the smooth representation of the polygon constraint, but several of these discretized nodes are not even near the restricted region, making these constraints unnecessary. An improvement would be to only add these constraints to the variables that are assumed to be affected by the restriction of the feasible region. It should also be noted that the constraints removing parts of the feasible region make the problem nonconvex. The optimizers used to solve the problem will only find a local minimum, making the solution depend on the initial starting guess. Finding the best solution would then be performed using a branch-and-bound technique to investigate all suitable solutions.

The formulation used here works well for a 2-D polygon, but including the altitude would turn the polygons into polytopes and an expansion to 3-D may be necessary. The expansion to 3-D has not been covered here because the altitude restrictions are too high in many cases, making it unlikely that the optimal solution would be flying above the region instead of around it.

Finding a suitable objective function is difficult. Minimizing the fuel burn makes the velocity rather low, but using other objectives in which flight idle is not beneficial, such as minimum time or some environmental index, has a tendency to make the solution oscillate quite drastically at the end to reduce the speed, instead of using a lower throttle setting. The oscillations are more related to modeling issues; however, a conclusion can be that efficient airbrakes could be beneficial if toxic emissions should be reduced close to airports, which will help the aircraft to make a steeper descent before landing. Also, when minimizing environmental indices, the shortest path is often optimal, if possible to fly; this may result in very steep turns, since the distance will be reduced.

Appendix A: Aircraft Data

The Saab 105 with Swedish Air Force (SAF) designation SK60 first flew in 1963 and is still used as the primary trainer in the SAF. The aircraft has continually been upgraded, including new engines in the mid-1990s. The aircraft was originally intended as a small business jet but has only been used in the SAF and the Austrian Air Force. The aircraft configuration involves a high wing with negative dihedral, a T-tail and two Williams FJ-44 turbojet engines. The basic aircraft data are listed in Table A1.

Table A1 Aircraft reference and aerodynamics data

Variable	Meaning	Value/Unit
S	Reference area	16.3 m^2
$\bar{c}$	Reference chord	1.7436 m
s	Span	9.5 m
h	Altitude	km
$C_{D0}(M)$	Basic drag coefficient	——
C_{Dh}	Altitude correction to drag	0.00028 km^{-1}
$C_{L\alpha}$	Lift slope	0.08 1/ deg
C_L^*	Shift in drag polar	0.05
C_{L0}	Lift at zero α	0.08
η	Induced drag coefficient	0.082
m	Mass with crew but no fuel	2876 kg
m_f	Maximum fuel mass	1118 kg

For efficient and reliable optimization, all aircraft data functions are implemented as smooth functions. For the Saab 105 model, this is achieved using a linear least-squares fit of B-spline basis functions to the original tabular data. For performance analysis and optimization, many aerodynamic coefficients can safely be treated as constants, even though the full model is a bit more elaborate. However, the basic drag coefficient needs to be modeled as function of the Mach number in the form

$$C_{D0}(M) = \sum_{i=1}^{n} a_i B_{i,l}(M) \tag{A1}$$

where $B_{i,l}$ are B-spline basis functions of order l. The resulting function is shown in Fig. A1. The remaining aerodynamic coefficients are listed in Table A1.

The coefficients are assembled into lift as

$$L = qS(C_{L0} + C_{L\alpha}\alpha) \tag{A2}$$

and the total drag as

$$D = qS(C_{D0} + C_{Dh}h + \eta(C_L - C_L^*)^2) \tag{A3}$$

where S is a reference area and q the dynamic pressure. The constant coefficient C_L^* is used to model the slight shift in the drag polar.

The thrust and fuel burn are modeled as three variable functions:

$$T(h, M, \delta_p) = \sum_{i=1}^{n_1}\sum_{j=1}^{n_2}\sum_{k=1}^{n_3} a_{ijk} B_{i,l}(h) B_{j,l}(M) B_{k,l}(\delta_p) \tag{A4}$$

where δ_p is the throttle. In all cases, the coefficients (for example a_{ijk}) are found by matching each B-spline model to tabular data by solving a least-squares problem.

The engine data are given for standard atmosphere (International Standard Atmosphere) conditions and three different throttle settings in Figs. A2–A7.

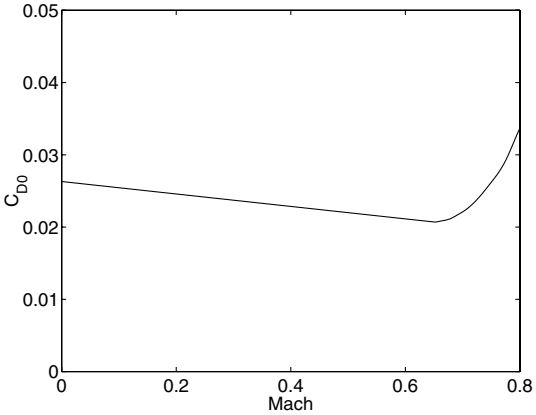

Fig. A1 Drag coefficient C_{D0}.

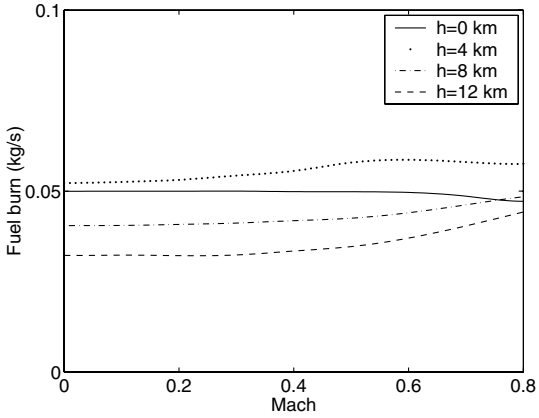

Fig. A2 Fuel burn at flight idle.

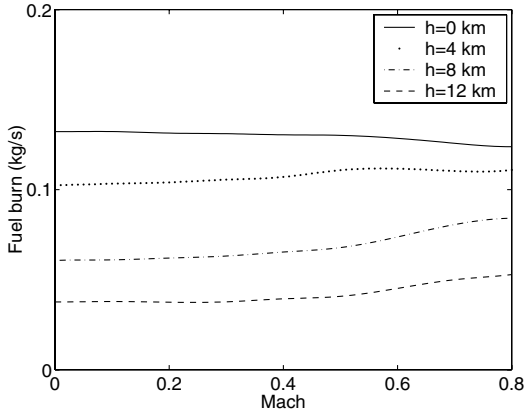

Fig. A3 Fuel burn at half throttle.

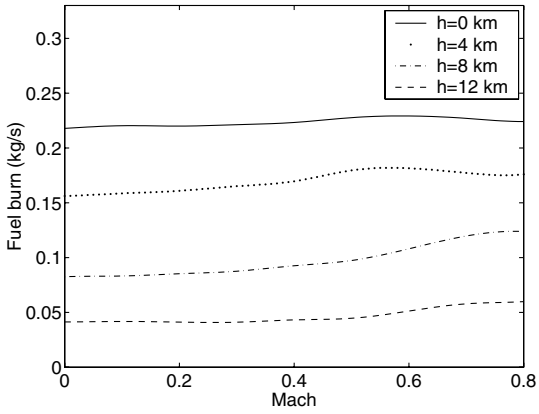

Fig. A4 Fuel burn at full throttle.

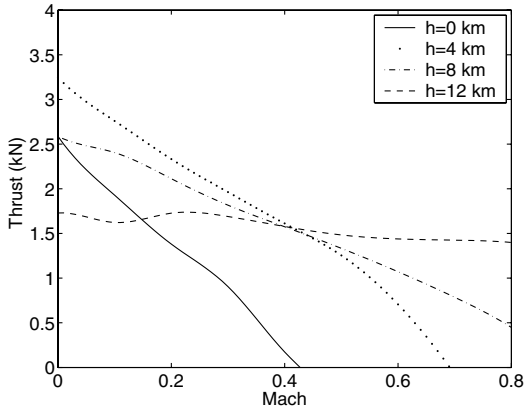

Fig. A5 Thrust at flight idle.

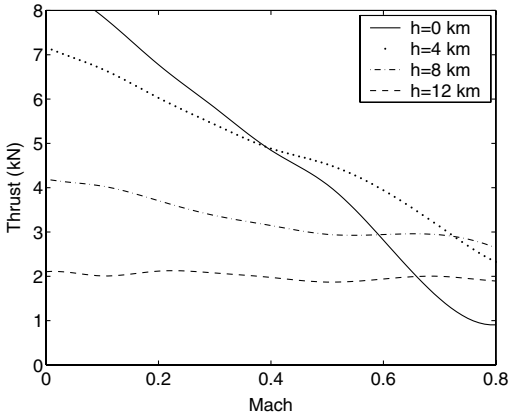

Fig. A6 Thrust at half throttle.

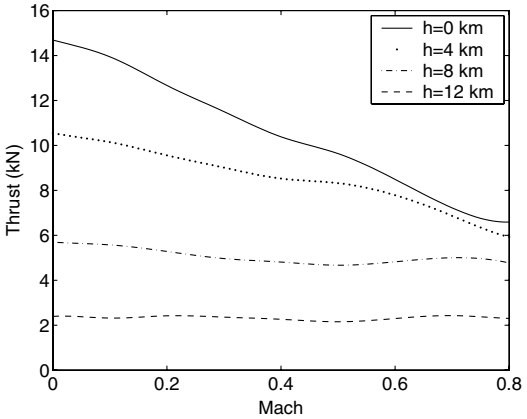

Fig. A7 Thrust at full throttle.

Acknowledgments

The authors are grateful for the development and support of SNOPT provided by Philip Gill at the University of California, San Diego, and by Walter Murray and Michael Saunders at Stanford University. The support by Mats Henningsson of the Swedish Air Force and Mats Axelsson, Lars Forsander, and Erik Prisell of the Swedish Defence Materiel Administration (FMV) is gratefully acknowledged. Special thanks to air traffic controller Magnus Carlsson for the information about approaches to Malmen airport.

References

[1] Hargraves, C. R., and Paris, S. W., "Direct Trajectory Optimization Using Nonlinear Programming and Collocation," *Journal of Guidance, Control, and Dynamics*, Vol. 10, No. 4, 1987, pp. 338–342. doi:10.2514/3.20223

[2] Ringertz, U. T., "Optimal Trajectory for a Minimum Fuel Turn," *Journal of Aircraft*, Vol. 37, No. 5, 2000, pp. 932–934. doi:10.2514/2.2697

[3] Norsell, M., "Multistage Trajectory Optimization with Radar-Range Constraints," *Journal of Aircraft*, Vol. 42, No. 4, 2005, pp. 849–857. doi:10.2514/1.8544

[4] Betts, J. T., "Very Low-Thrust Trajectory Optimization Using a Direct SQP Method," *Journal of Computational and Applied Mathematics*, Vol. 120, 2000, pp. 27–40. doi:10.1016/S0377-0427(00)00301-0

[5] Tsuchiya, T., Ishii, H., Uchida, J., Ikaida, H., Gomi, H., Matayoshi, N., and Okuno, Y., "Flight Trajectory Optimization to Minimize Ground Noise in Helicopter Landing Approach," *Journal of Guidance, Control, and Dynamics*, Vol. 32, No. 2, 2009, pp. 605–615. doi:10.2514/1.34458

[6] Betts, J. T., *Practical Methods for Optimal Control Using Nonlinear Programming*, Advances in Design and Control, Society for Industrial and Applied Mathematics, Philadelphia, 2001.

[7] Jorris, T. R., and Cobb, R. G., "Three-Dimensional Trajectory Optimization Satisfying Waypoint and No-Fly Zone Constraints,"

Journal of Guidance, Control, and Dynamics, Vol. 32, No. 2, 2009, pp. 551–572.
doi:10.2514/1.37030

[8] Eele, A., and Richards, A., "Path-Planning with Avoidance Using Nonlinear Branch-and-Bound Optimization," *Journal of Guidance, Control, and Dynamics*, Vol. 32, No. 2, 2009, pp. 384–394.
doi:10.2514/1.40034

[9] Dai, R., and Cochran, J. E., Jr., "Three-Dimensional Trajectory Optimization in Constrained Airspace," *Journal of Aircraft*, Vol. 46, No. 2, 2009, pp. 627–634.
doi:10.2514/1.39327

[10] Etkin, B., and Reid, L. D., *Dynamics of Flight, Stability and Control*, Wiley, New York, 1996.

[11] de Boor, C., "Package for Calculating with *B*-Splines," *SIAM Journal on Numerical Analysis*, Vol. 14, No. 3, June 1977, pp. 441–472.
doi:10.1137/0714026

[12] Ringertz, U., "Aircraft Trajectory Optimization as a Wireless Internet Application," *Journal of Aerospace Computing, Information, and Communication*, Vol. 1, No. 2, 2004, pp. 85–99.
doi:10.2514/1.1279

[13] *ICAO Engine Emissions Databank* [online database], Civil Aviation Authority, West Sussex, England, U.K., http://www.caa.co.uk/default.aspx?catid=702&pagetype=68 [retrieved 30 July 2009].

[14] DuBois, D., and Paynter, G. C., "Fuel Flow Method 2 for Estimating Aircraft Emissions," SAE International Paper 2006-01-1987, 2006.

[15] Baumann, H., and Tillman, A., *The Hitch Hiker's Guide to LCA*, Studentlitteratur, 2004.

[16] Goedkoop, M., and Spriensma, R., "The Eco-indicator'99: A Damage Oriented Method for Life Cycle Impact Assessment," PRé Consultants, Amersfoort, The Netherlands, 1999.

[17] Brenan, K. E., "Differential-Algebraic Equations Issues in the Direct Transcription of Path Constrained Optimal Control Problems," Rept. ATR-94(8489)-1, The Aerospace Corp., El Segundo, CA, Dec. 1993.

[18] Ringertz, U. T., "Multistage Trajectory Optimization Using Large-Scale Nonlinear Programming," TR 99-25, Royal Inst. of Technology, Dept. of Aeronautical and Vehicle Engineering, Stockholm, 1999.

[19] Gill, P. E., Murray, W., and Saunders, M. A., "SNOPT: An SQP Algorithm for Large-Scale Constrained Optimization," *SIAM Review*, Vol. 47, No. 1, 2005, pp. 99–131.
doi:10.1137/S0036144504446096

[20] Judd, K. B., and McLain, T. W., "Spline Based Path Planning for Unmanned Air Vehicles," AIAA Guidance, Navigation, and Control Conference and Exhibit, AIAA Paper 2001-4238, Montreal, Aug. 2001.

[21] Norsell, M., "Aircraft Trajectory Optimization with Tactical Constraints," Ph.D. Thesis, Royal Inst. of Technology, Stockholm, 2004.

[22] Jorris, T. R., Schultz, C. S., Friedl, F. R., and Rao, A. V., "Constrained Trajectory Optimization Using Pseudospectral Methods," AIAA Atmospheric Flight Mechanics Conference and Exhibit, AIAA Paper 2008-6218, Honolulu, HI, Aug. 2008.

[23] Xu, S., Freund, R. M., and Sun, J., "Solution Methodologies for the Smallest Enclosing Circle Problem," *Computational Optimization and Applications*, Vol. 25, Nos. 1–3, 2003, pp. 283–292.
doi:10.1023/A:1022977709811

[24] Kumar, P., and Yildirim, E. A., "Minimum-Volume Enclosing Ellipsoids and Core Sets," *Journal of Optimization Theory and Applications*, Vol. 126, No. 1, 2005, pp. 1–21.
doi:10.1007/s10957-005-2653-6

[25] Khachiyan, L. G., "Rounding of Polytopes in the Real Number Model of Computation," *Mathematics of Operations Research*, Vol. 21, No. 2, 1996, pp. 307–320.
doi:10.1287/moor.21.2.307

[26] Raghunathan, A. U., Gopal, V., Subramanian, D., Biegler, L. T., and Samad, T., "3-D Conflict Resolution of Multiple Aircraft via Dynamic Optimization," AIAA Guidance, Navigation, and Control Conference and Exhibit, AIAA Paper 2003-5675, Austin, TX, Aug. 2003.

[27] *M_Map: A Mapping Package for MATLAB*, http://www.eos.ubc.ca/~rich/map.html [retrieved 30 July 2009].

[28] Guinée, J., "Life Cycle Assessment: An Operational Guide to the ISO Standards," Centre of Environmental Science, Leiden Univ., Leiden, The Netherlands, 2002.